scientific reports

Check for updates

OPEN

Cloning of *nf-profilin* and intercellular interaction with *nf-actin* in *Naegleria fowleri* cysts

Hae-Jin Sohn[1], A-Jeong Ham[1], A-Young Park[1], Jeong-Heon Lee[1], Sun Park[1], Ho-Joon Shin[1] & Jong-Hyun Kim[2]✉

Naegleria fowleri **is a free-living amoeba found in lakes, soil, hot springs, and poorly chlorinated swimming pools. It is pathogenic to humans, causing a rare and fatal brain infection known as primary amoebic meningoencephalitis (PAM). A previous study utilized RNA-seq analysis to examine genes expressed in *N. fowleri* cysts and trophozoites, focusing on the *nf-profilin* gene, which showed high expression in cysts. Profilin is a small actin-binding protein that regulates *nf-actin* polymerization and cell movement. Sequence analysis revealed 83% similarity with non-pathogenic *N. gruberi* and 38% similarity with *Acanthamoeba castellanii*. Nf-profilin was found to be associated with *N. fowleri* lysates but not with lysates from other amoebae, as shown by Western blot analysis. Immunofluorescence assays demonstrated that *nf-profilin* primarily localized to the cell membrane in *N. fowleri* cysts, while *nf-actin* localized to the cytoplasm, pseudopodia, and food-cup structures. Real-time RT-PCR indicated higher expression of the *nf-profilin* gene in cysts compared to trophozoites. In co-culture experiments with target cells, Nf-profilin was initially expressed in the cytoplasm of *N. fowleri* cysts and the morphology of cyst gradually transitioned to the trophozoite form. Concurrently, the expression of Nf-profilin protein decreased, while Nf-actin protein began to appear in the pseudopodia and food-cups of trophozoites. In conclusion, the *nf-profilin* and *nf-actin* genes exhibited complementary expression patterns based on the life stage of *N. fowleri*, indicating their critical roles in the survival and proliferation. This study emphasizes the significance of actin-binding proteins in understanding the infection and pathogenic mechanisms of *N. fowleri*.**

Keywords *Naegleri fowleri*, Actin-binding protein, Profilin, Pathogenicity mechanisms

Naegleria fowleri is a free-living amoeba commonly found in warm freshwater environments such as lakes, rivers, hot springs, and poorly chlorinated swimming pools[1,2]. *N. fowleri* is a thermophilic pathogenic amoeba that thrives at 37 °C but can survive in higher temperatures, up to approximately 45 °C[3,4]. The rise in global temperatures is expanding *N. fowleri* habitat and population due to its preference for warmer environments[5,6].

The life cycle of *N. fowleri* consists of three stages: trophozoite, flagellate, and cyst. The cyst stage is a dormant form that enables the organism to survive harsh environmental conditions. In contrast, the active trophozoite form can enter the human body through the nasal passage, leading to severe brain infections[4,7,8]. When contaminated water enters the nasal passage during activities like swimming or diving, the amoeba can travel along the olfactory nerve to the brain. This pathogen can cause a rare and severe brain infection called primary amoebic meningoencephalitis (PAM)[9]. PAM progresses rapidly and is often fatal, with symptoms including severe headache, fever, nausea, vomiting, stiff neck, confusion, seizures, and coma. With a mortality rate of approximately 97%, the disease is difficult to diagnose due to its resemblance to bacterial or viral meningitis[10]. While treatments like Amphotericin B or Miltefosine are used to manage PAM, no fully effective treatment currently exists[11–13]. Preventing exposure by keeping contaminated water from entering the nasal passages remains the primary method of avoiding *N. fowleri* infection[7]. Thus, rapid diagnosis and treatment are critical to improving survival rates.

The pathogenic mechanisms of *N. fowleri* are not well understood. Previous research suggests that a cytopathic effect induces cell death after amoeba-host cell contact[7]. *N. fowleri* invades the central nervous system (CNS) through the olfactory nerve and destroys brain tissue, forming structures called amoebastomes or food-cups[14]. Additionally, *N. fowleri* adheres to host cells via fibronectin and integrin-like proteins, with

[1]Department of Microbiology, Ajou University School of Medicine, Suwon 16499, Republic of Korea. [2]Institute of Animal Medicine, College of Veterinary Medicine, GNU (Gyeongsang National University), Jinju 52828, Republic of Korea. ✉email: jkim@gnu.ac.kr

involvement from protease kinase C[15,16]. The pathogenic mechanisms of *N. fowleri* are thought to involve two main processes: contact-dependent and contact-independent. In the contact-dependent process, the amoeba attaches to target cells, leading to their destruction, with genes such as *nfa1*, *nf-hsp70*, and *nf-actin* playing key roles in pathogenicity[14,17–20]. In the contact-independent process, *N. fowleri* secretes proteins that damage target cells such as phospholipase, secretion of proteases and extracellular secreted proteins (ESP)[9,21,22].

In previous studies, we analyzed genes differentially expressed in *N. fowleri* trophozoites and cysts using RNA-seq [23]. These studies revealed proteins involved in differentiation, growth, and cell death during cyst formation. In this study, we focused on the differential expression of *nf-profilin* during amoebic life stages and examined the correlation between *nf-profilin* and *nf-actin* in target cells. Profilin is an important small actin-binding protein that regulates the cytoskeleton and cell movement[24,25]. It binds to G-actin (monomeric actin) and regulates the polymerization of F-actin (actin filaments)[14,26]. Additionally, profilin interacts with various proteins involved in cytoskeletal organization, membrane dynamics, and signal transduction pathways, contributing to its diverse cellular functions[27,28]. Actin, a cytoskeletal protein, plays a key role in actin polymerization, triggered by structural changes and external stimuli, and it forms food-cups during the phagocytic process[14,20,29,30]. Based on this, we observed differential *nf-profilin* expression during the amoebic life cycle. We also examined the expression levels and correlation of *nf-profilin* and *nf-actin* in target cells using fluorescence microscopy. This data will be crucial for understanding the pathogenic mechanisms underlying fatal primary amoebic meningoencephalitis.

Results

Expression of the *nf-profilin* gene during cyst formation

To induce encystation, we modified the previously reported method[31]. *N. fowleri* was starved for 18 h in incomplete Nelson's medium to induce cyst formation, after which the medium was replaced with encystment medium. Microscopy showed that the amoebae's vacuoles expanded, their pseudopodia disappeared, and they transformed into a rounded shape. Most *N. fowleri* cells formed precysts, and cyst formation was observed (Fig. 1). We investigated the expression of the *nf-profilin* gene in *N. fowleri* trophozoites and cysts. Total RNA was isolated, and cDNA was synthesized. RT-PCR analysis showed that the *nf-profilin* gene (450 bp) was more highly expressed during cyst formation (Fig. 2). In contrast, pathogenesis-related genes, such as *nfa1* and *nf-actin*, exhibited higher expression in trophozoites. The *nae3* gene is the 18 S rRNA of *N. fowleri* and the primer used to identify of *N. fowleri*. The *nae3* and *nf-gapdh* genes were used as controls.

Characterization and homology analysis of the *nf-profilin* gene

The open reading frame (ORF) of the *nf-profilin* gene is 450 bp and encodes a 150 amino acid protein with a predicted molecular weight of 16.5 kDa (Fig. 3). No introns were found in the *nf-profilin* gene in the genomic DNA of *N. fowleri*. Homology analysis revealed that the *nf-profilin* gene is conserved from protozoa to humans (Table 1). The deduced amino acid sequence of *nf-profilin* gene showed 83% homology with non-pathogenic *N. gruberi*, 33% homology with *Acanthamoeba castellanii*, and 18% homology with human *profilin* gene (Table 1). Recombinant Nf-profilin-(His) fusion protein was expressed in *E. coli* as a 22.5 kDa recombinant protein and purified (Fig. 4). Cross-reactivity tests using *N. fowleri* cyst lysates with anti-mouse Nf-profilin antibodies demonstrated specific reactivity with *N. fowleri* cysts but not with *Acanthamoeba* spp. lysates (Fig. 4).

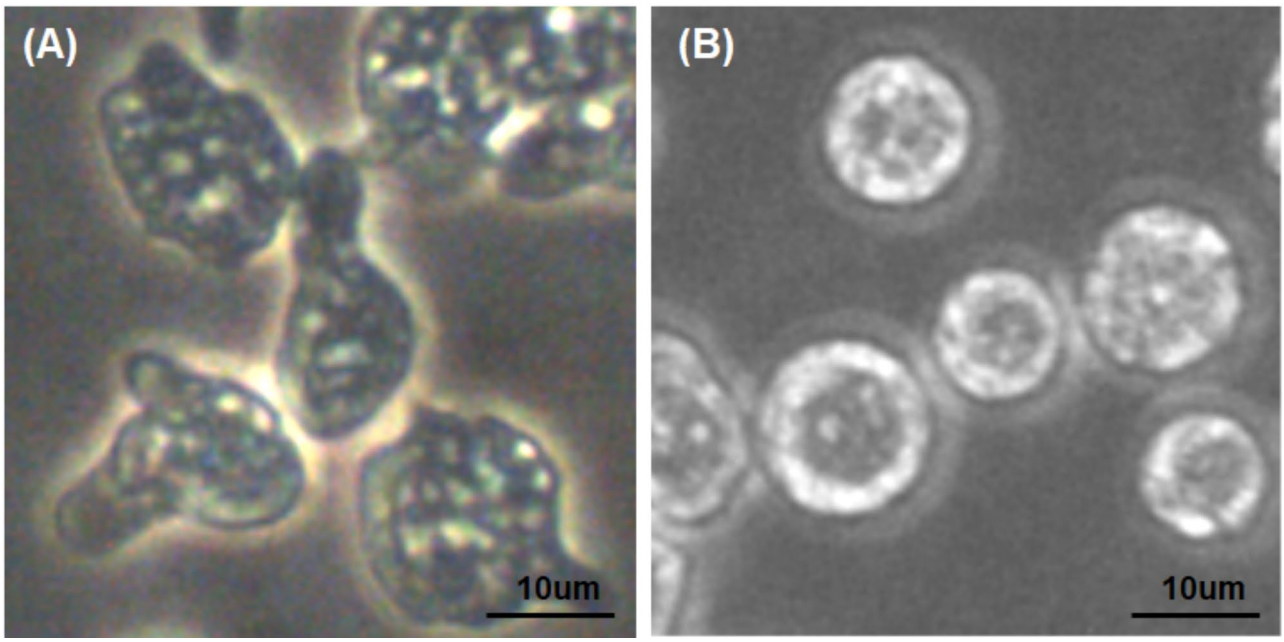

Fig. 1. Live image of *N. folweri* (**A**) trohpozoites and (**B**) encystic forms (× 200).

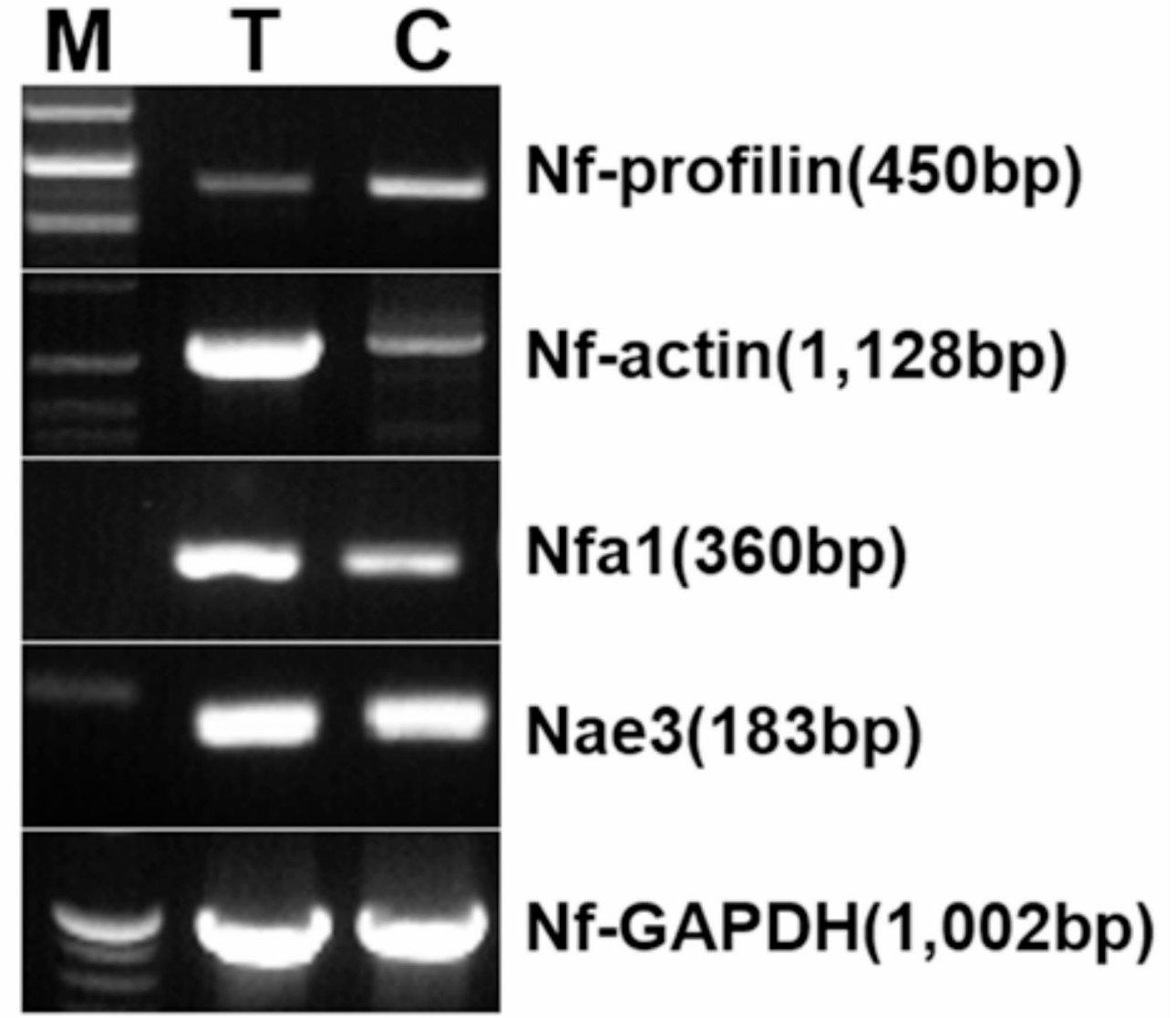

Fig. 2. *Nf-profilin* and *nf-actin* gene expression level of *N. foweleri* trophozoites and cysts. T, *N. fowleri* trophozoites; C, *N. fowleri* cysts; *nfa1*, pseudopodia-specific gene of *N. fowleri*; *Nae3* and *Nf-GAPDH* were used for the control genes. M; DNA size marker.

Cellular localization of Nf-profilin

The localization of Nf-profilin protein in *N. fowleri* trophozoites and cysts was examined using an immunofluorescence assay (Fig. 5). The expression of Nf-profilin is shown in green color (FITC); it is more prominently marked in *N. fowleri* cysts compared to *N. fowleri* trophozoites. Nf-profilin was strongly expressed in the cytoplasm of *N. fowleri* cysts, while in trophozoites, it was weakly expressed at the cell membrane and the tips of pseudopodia. In contrast, Nf-actin was strongly expressed in amoebastomes (food-cup formations) of trophozoites but weakly expressed in the cytoplasm of cysts (Fig. 6).

Differential expression of Nf-profilin in *N. fowleri* co-cultured with CHO cells

N. fowleri cysts and trophozoites were co-cultured with CHO cells to observe morphological changes and phagocytosis (Fig. 7). The number of CHO cells decreased and became rounded as the co-culture progressed. In experimental group II, where *N. fowleri* cysts were co-cultured with CHO cells, the cysts were initially observed floating near the CHO cells and transitioning to a pre-cyst form after 3 h. By 6 h, the cysts had excysted and transformed into trophozoites. After 12 h, the trophozoites were observed actively destroying the CHO cells. By 24 h, no cysts remained, and the number of CHO cells had significantly decreased (Fig. 7). In experimental group I, where *N. fowleri* trophozoites were co-cultured with CHO cells, phagocytosis began within 1 h, and the number of amoebae increased, eventually surpassing the number of CHO cells (Fig. 7). We also synthesized cDNA and performed RT-PCR to determine the expression level of the *nf-profilin* gene during co-culture (Fig. 8). In experimental group I, *nf-profilin* expression remained low throughout the co-culture (~24 h). In

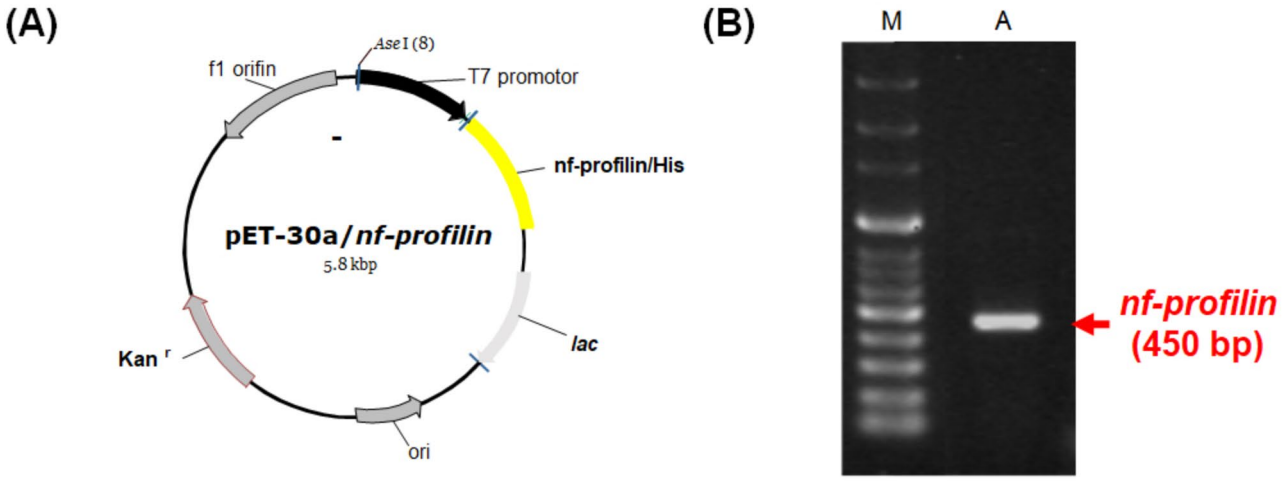

Fig. 3. (**A**) Construction of expression vector. The pET-30a vector containing His-tag. Cloning of *nf-profilin* gene into the pET-30a vector. (**B**) Amplified PCR product of *nf-profilin gene* of pET-30a/*nf-profilin*. M, DNA size marker; lane A, amplified PCR product of *nf-profilin* gene of pET-30a/*nf-profilin*.

Other species	Percentage of Identity (%)	
profilin [*Naegleria gruberi* strain NEG-M]	83	Non-pathogenic amoeba
Acanthamoeba castellanii str. Neff profilin	33	Other amoeba spp.
Entamoeba histolytica profilin	38	Protozoa
Human gene for profilin	18	Human

Table 1. Identity with *profilin* gene amino acid sequence of other species.

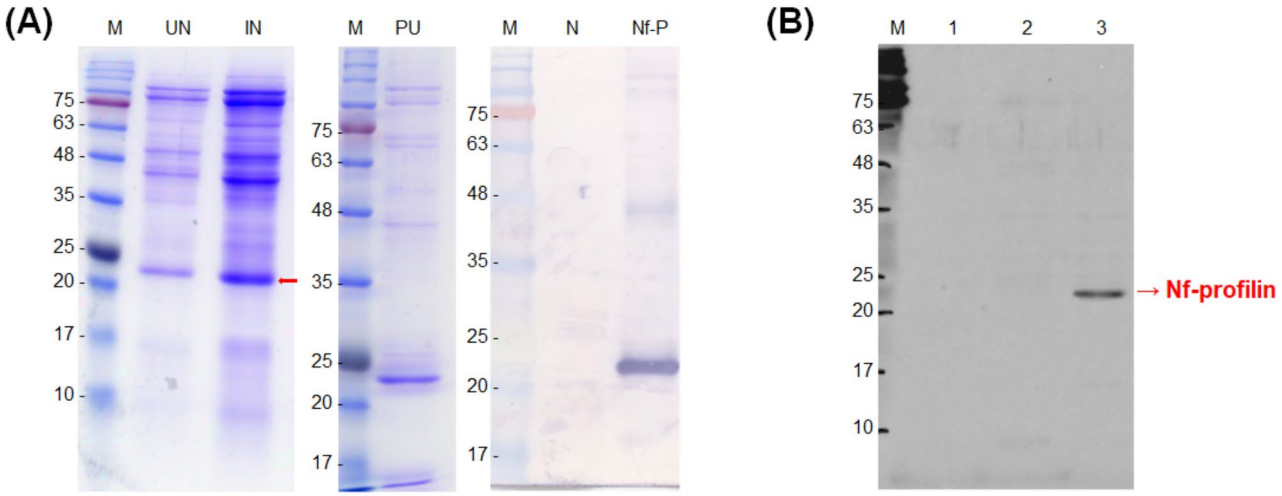

Fig. 4. (**A**) Band patterns of SDS-PAGE and Western blot of the IPTG-induced recombinant protein (Nf-profilin). M, molecular weight marker; UN, uninduced *E. coli* lysate, IN, IPTG induced *E. coli* lysate; PU, purified recombinant Nf-profilin protein using Ni-NTA resin; N, normal mouse sera (1:1000); Nf-P, anti-Nf-profilin antibody (1:1000). (**B**) Cross reactivity of anti-Nf-profilin antibody. lane 1, *A. castellanii*; lane 2, *A. polyphaga*; lane 3, *N. fowleri*.

contrast, experimental group II showed the highest expression of *nf-profilin* after 1 h of co-culture, followed by a decrease in expression at 3 h, which remained low for the remainder of the 24 h period. Conversely, *nf-actin* and *nfa1* were highly expressed in trophozoites and were not significantly affected by co-culture duration. Quantitative real-time PCR analysis revealed that after 6 h of co-culture, there was no significant difference in *nf-profilin* expressions in trophozoites or cysts, respectively (Fig. 9). However, in experimental group II, *nf-profilin*

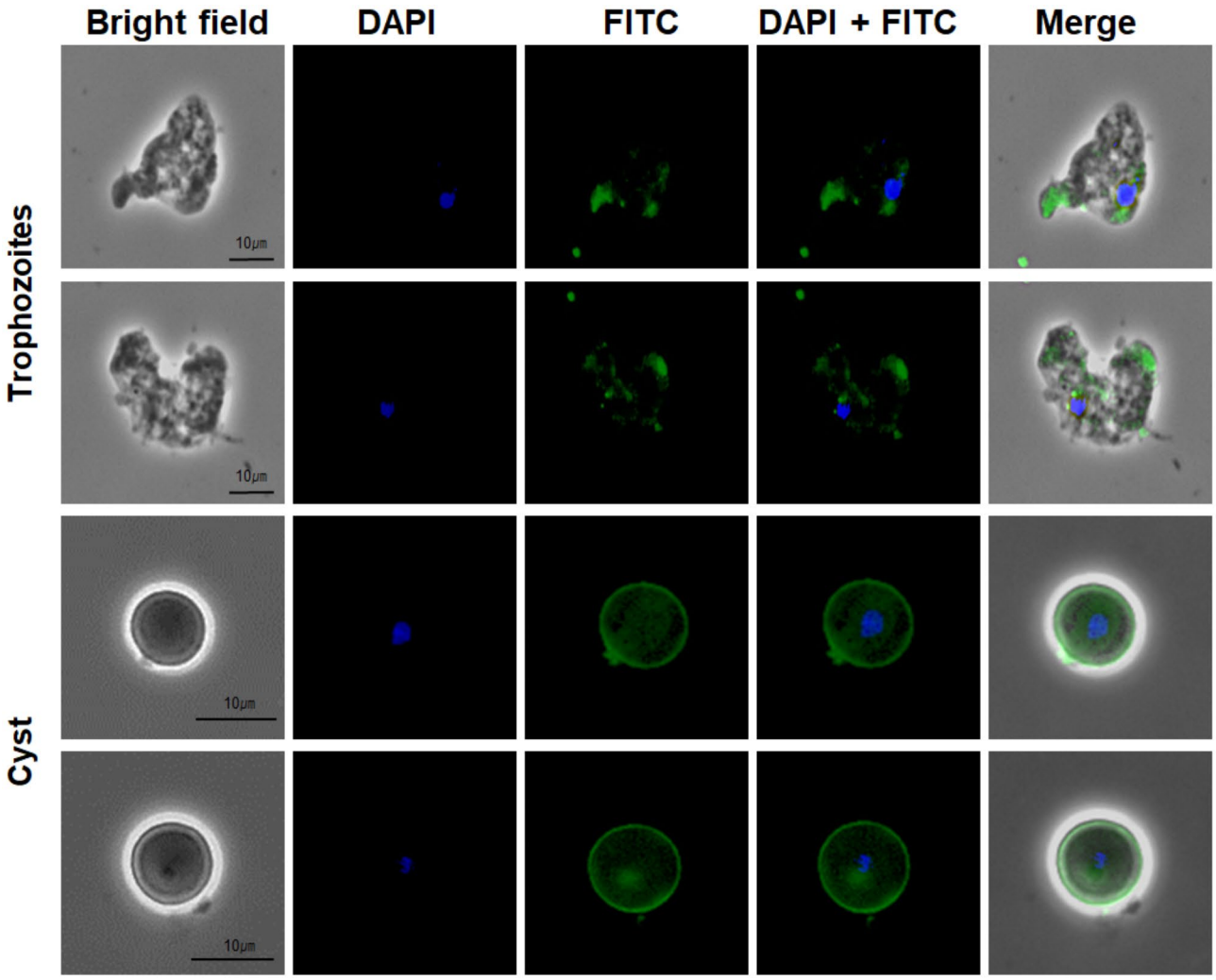

Fig. 5. Cellular expression of the Nf-profilin in trophozoites and cysts by immunofluorescence assay. The light microscopic findings were shown in the inner box (× 400). Upper panels, *N. fowleri* trophozoites; Lower panels, *N. fowleri* cysts. Scale bar, 10 μm.

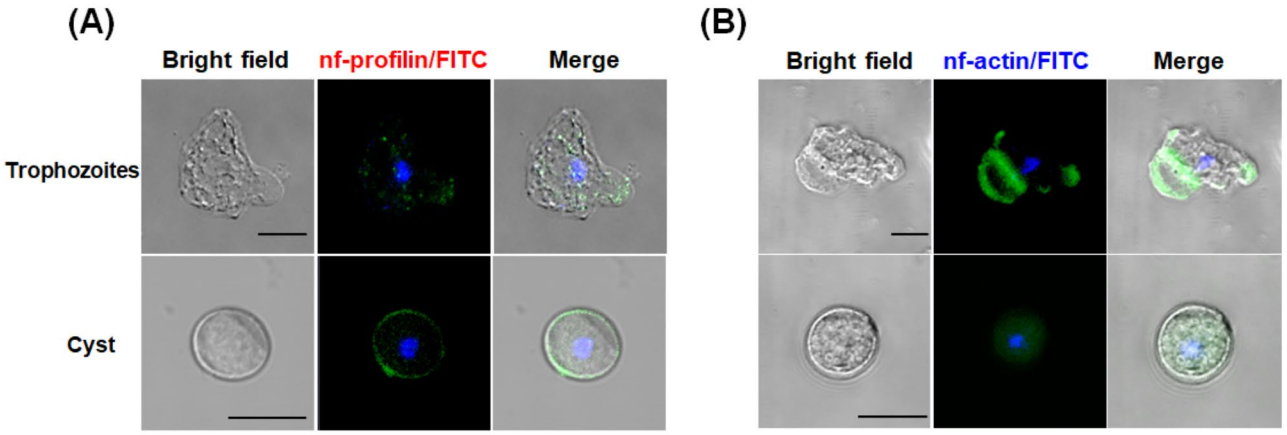

Fig. 6. Localization of (**A**) Nf-profilin and (**B**) Nf-actin in trophozoites and cysts by confocal microscope. Green fluorescence (FITC) indicates Nf-profilin or Nf-actin, and blue fluorescence (DAPI) indicates cell nuclei. The bright fields were shown in the inner box (× 800). Upper panels, *N. fowleri* trophozoites; Lower panels, *N. fowleri* cysts. Scale bar, 10 μm.

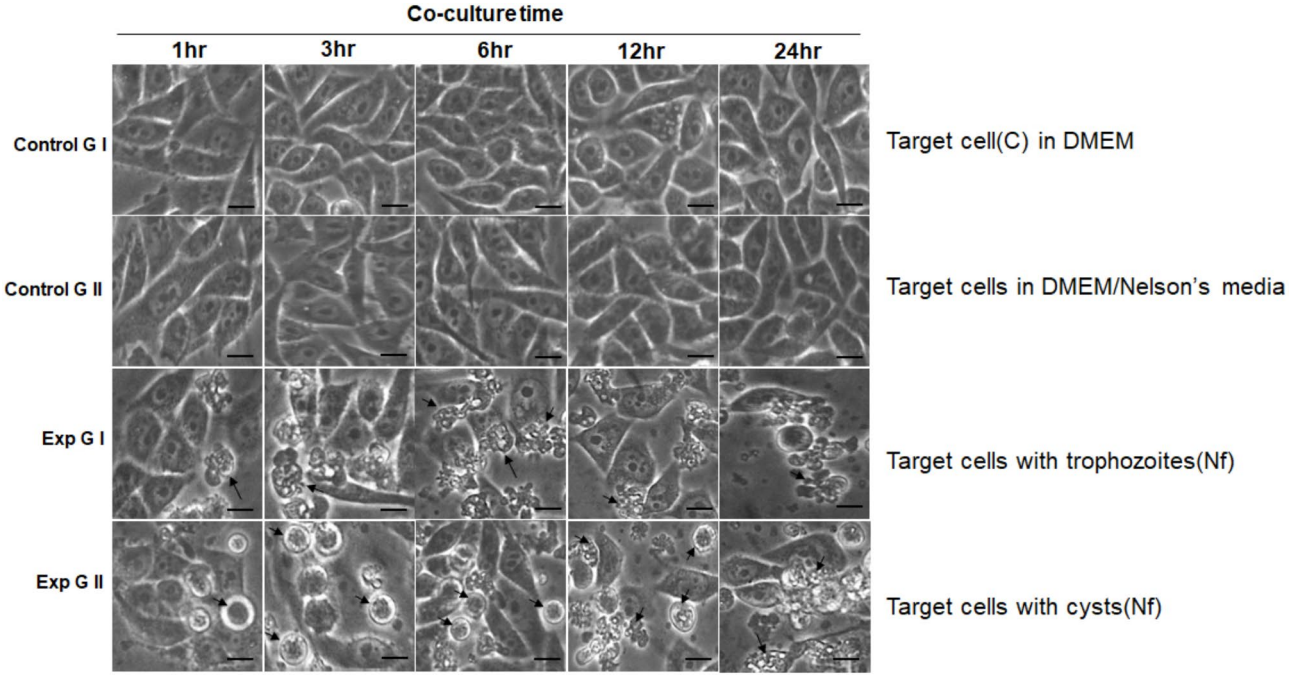

Fig. 7. Microscopic observation of *N. fowleri* co-cultured with CHO cells. Control G I, CHO cells in DMEM; Control G II, CHO cells in DMEM mixed with Nelson's medium; Exp G I, CHO cells with *N. fowleri* trophozoites; Exp G II, CHO cells with *N. fowleri* cysts (× 400). Arrow, *N. fowleri*, Scale bar, 20 μm.

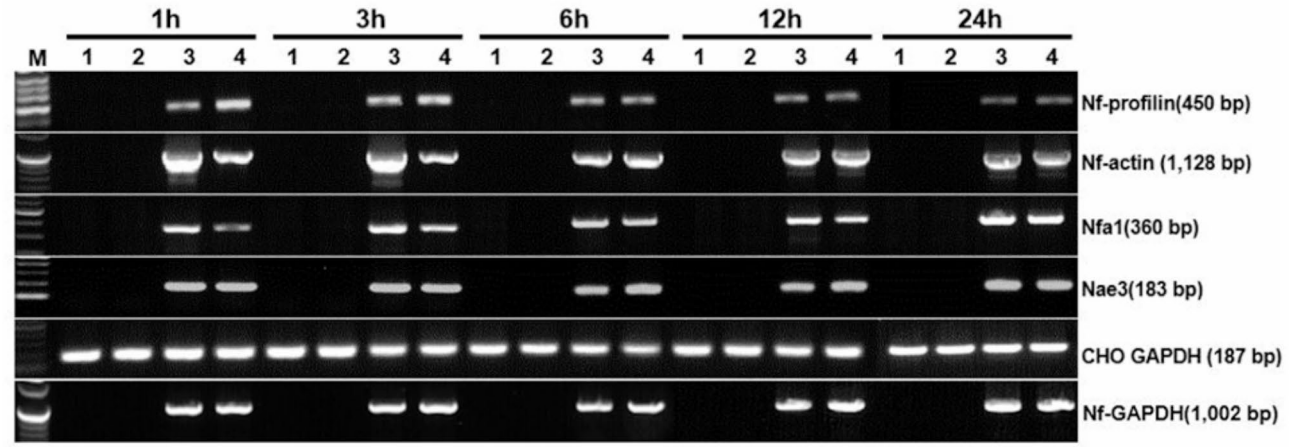

Fig. 8. *Nf-profilin* gene expression levels in *N. fowleri* co-cultured with CHO cells using RT-PCR. lane 1, CHO cells in DMEM (Control G I); lane 2, CHO cells in mixture medium with DMEM and Nelson's medium (Control G II); lane 3, CHO cells with *N. fowleri* trophozoites (Exp G I); lane 4, CHO cells with *N. fowleri* cysts (Exp G II). The *nf-actin* and *nfa1* genes were used for the trophozoite-dominant gene, CHO GAPDH, Nf-GAPDH and *Nae3* genes were used for the controls. M, DNA size marker.

expression (4.124) was 2.5 times higher than in experimental group I (1.608) after 1 h of co-culture ($p < 0.05$) (Fig. 9). *Nf-profilin* expression remained constant after 6 h in experimental group II, showing a similar pattern to experimental group I. The results were analyzed using the comparative 2-ΔΔCT method, which normalizes the CT value of Nf-GAPDH as a control and compares it to the CT value of *nf-profilin* gene.

Localization of Nf-profilin protein in *N. fowleri* co-cultured with CHO cells

We further investigated *nf-profilin* expression in *N. fowleri* trophozoites and cysts co-cultured with CHO cells using immunofluorescence assays. As shown Fig. 10 (*N. fowleri* cysts co-cultured with CHO cells), Nf-profilin was localized in the cytoplasm of *N. fowleri* cysts near the CHO cells after 1 h of co-culture. After 3 h, cysts developed pseudopodia and vacuoles, with Nf-profilin concentrated inside the rounded amoebae or at the

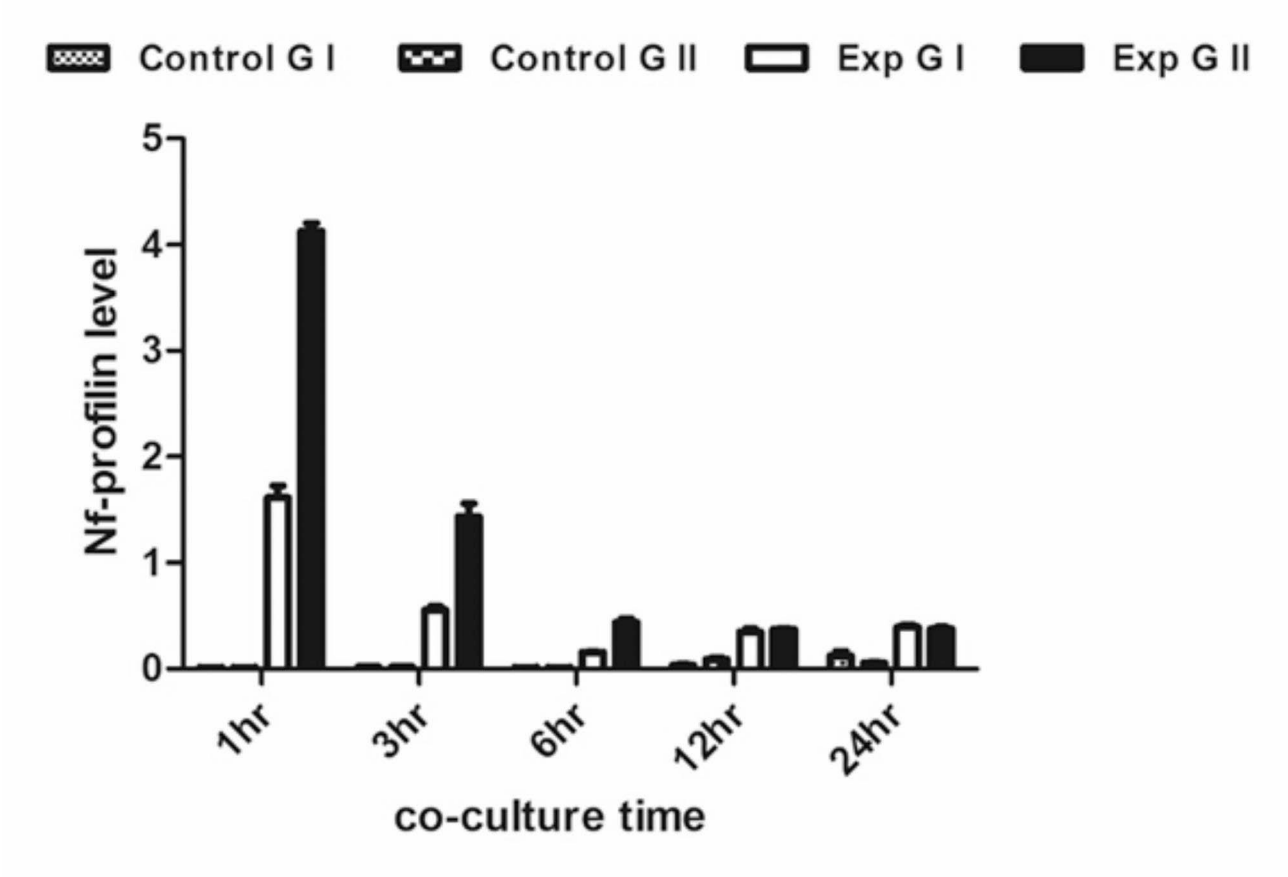

Fig. 9. *Nf-profilin* gene expression level of *N. fowleri* co-cultured with CHO cells using quantitative RT-PCR analysis. Control G I, CHO cells in DMEM; Control G II, CHO cells in DMEM mixed with Nelson's medium; Exp G I, CHO cells with *N. fowleri* trophozoites; Exp G II, CHO cells with *N. fowleri* cysts.

ends of pseudopodia. After 6 h, *N. fowleri* had fully transformed into trophozoites with pseudopodia and food-cup formations. Some trophozoites showed multiple nuclei, and Nf-profilin expression decreased, primarily localizing inside the amoebae (Fig. 10). By 12 h, *N. fowleri* trophozoites had adhered to and engulfed the CHO cells, leading to the disruption of the CHO cells. Nf-profilin expression was minimal, primarily at the tips of pseudopodia or within the trophozoites. In contrast, Nf-profilin expression remained consistently low in experimental group I (*N. fowleri* trophozoites co-cultured with CHO cells) (Fig. 11).

Additionally, we observed the expression of Nf-actin protein, which is related to Nf-profilin. In experimental group II (*N. fowleri* cysts co-cultured with CHO cells), Nf-actin expression was very weak at 1 h (Fig. 12). However, once amoebastomes (food-cup formations) began to develop at 3 h, Nf-actin was distributed throughout the cytoplasm, with strong expression in the food-cups. By 6 h, *N. fowleri* cysts had almost fully transitioned into trophozoites, and Nf-actin expression was strongly localized in the food-cups of amoebae attached to CHO cells (Fig. 12). In contrast, in experimental group I (*N. fowleri* trophozoites co-cultured with CHO cells), Nf-actin was strongly expressed in trophozoites attached to CHO cells, showing phagocytic activity from the 1 h mark (Fig. 13). As co-culture time increased, the number of target cells decreased or ruptured due to trophozoites activity.

Discussion

N. fowleri, which is ubiquitous, often infects humans through the nasal or olfactory nerve during water activities[32]. Reports indicate that *N. fowleri* has been found in tap water. In a 2020 CDC study, *N. fowleri* was discovered in 3 out of 11 tap water samples in Texas, leading to the declaration of a disaster zone[33]. Recent global warming and rising temperatures have expanded the habitats of *N. fowleri*, potentially resulting in an increased incidence of infections[34]. PAM exhibits clinical symptoms that closely resemble those of viral or bacterial meningitis, complicating accurate diagnosis. Therefore, early diagnosis is difficult, yet essential for prompt treatment.

Based on previous studies, we can propose the following hypotheses regarding the pathogenic mechanisms of *N. fowleri*: (1) Contact-independent mechanism – *N. fowleri* secretes proteins that damage target cells[21]; (2) Contact-dependent mechanisms – *N. fowleri* produces genes involved in the development of amoebastomes or food-cups, leading to the destruction of target cells[20,35]. The *nfa1* gene related to this process is reported to be specifically expressed in the pseudopodia[19]. Additionally, the *hsp70* gene has been identified as a molecular chaperone involved in the formation of food-cups[36]. The cytoskeletal protein, Nf-actin, is associated with the

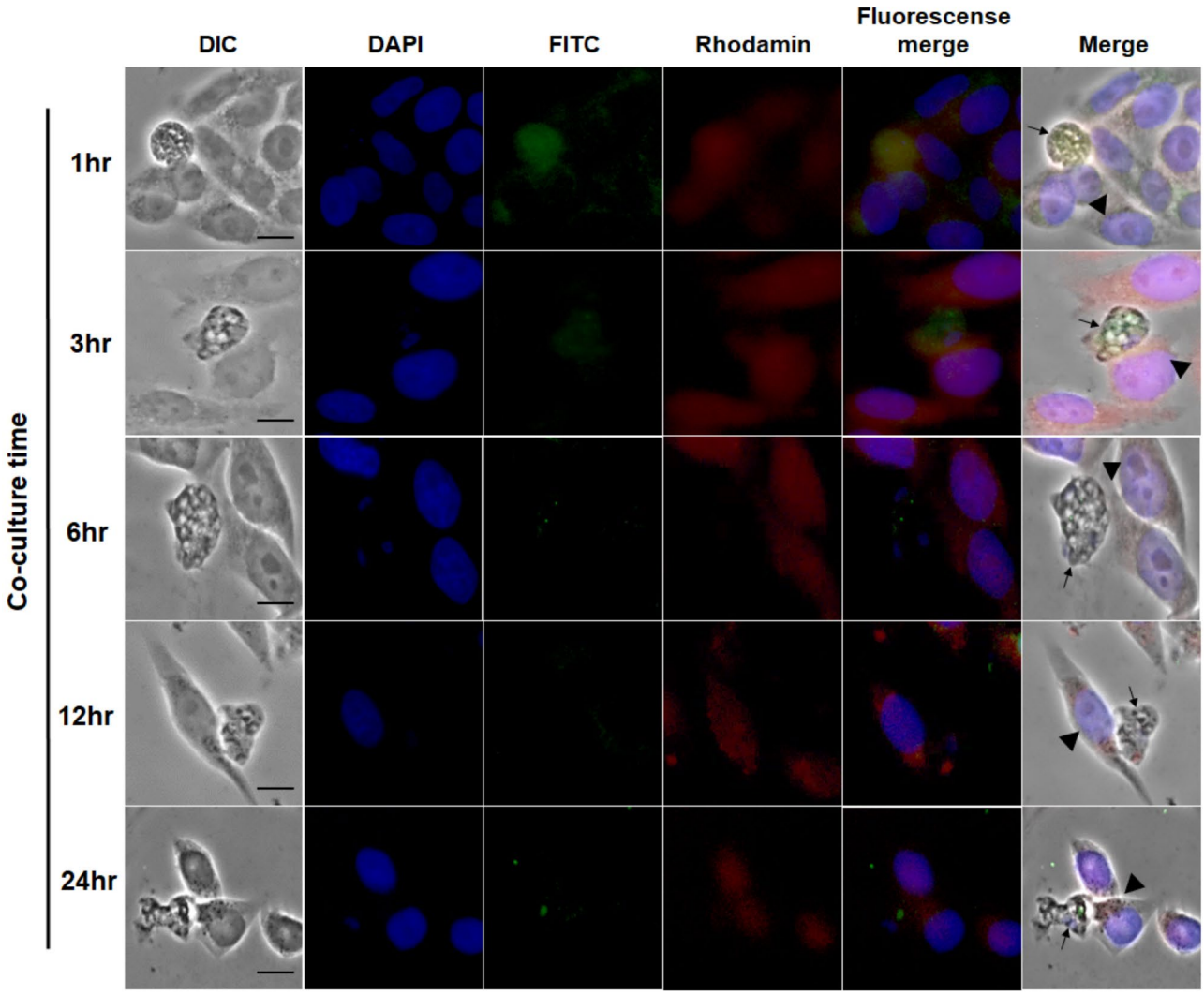

Fig. 10. Localization of Nf-profilin protein in *N. fowleri* cysts co-cultured with CHO cells by immunofluorescence assay (× 400). Arrow, *N. fowleri* cysts and trophozoites; Arrow head, CHO cells. Scale bar, 20 μm.

polymerization of fibrillar actin (F-actin) and globular actin (G-actin) and is highly expressed in the food-cup during phagocytosis[14,20].

N. fowleri consists of a nucleus and cytoplasm and contains various organelles, including food vacuoles, contractile vacuoles, and cytoplasmic vacuoles. Additionally, *N. fowleri* undergoes encystation, a process during which it transitions from the trophozoites to the cysts in response to environmental stress or adverse conditions. Cyst formation is recognized as an important factor that reduces the effectiveness of treatment[37]. The cyst form has limited many functions required for pathogenicity, including migration, division, and phagocytosis, compared to the trophozoite form. We propose that identifying the mechanisms that inhibit cyst-related genes would greatly contribute to understanding the pathogenicity of the amoebae. Recently, we conducted a transcriptome analysis of *N. fowleri* trophozoites and cysts using RNA-seq [23]. Our findings revealed that *nf-profilin* is highly expressed in the cyst stage of *N. fowleri*. The profilin is known to be a small actin-binding protein that plays a crucial role in regulating the actin cytoskeleton by promoting the exchange of ADP for ATP in G-actin, thereby facilitating actin filament assembly (F-actin)[38–40]. It also interacts with various proteins involved in cellular processes such as cell migration, division, and membrane trafficking, contributing to essential functions like wound healing and maintaining cell shape[29,30]. As a follow-up to these findings, we designed a study to clone and characterize *nf-profilin*, as well as to investigate the intercellular interaction between *nf-profilin* and *nf-actin*. Our experimental approach consisted of first cloning and characterizing *nf-profilin*, then observing its expression in two stages of *N. fowleri* (trophozoites and cysts), and finally examining its intercellular interaction with *nf-actin*.

This study compared *nf-profilin* gene expression levels between *N. fowleri* trophozoites and cysts and analyzed amoebic phagocytic activity and morphological changes through separate co-culture experiments with CHO cells. The *nf-profilin* gene, with a 450 bp coding sequence, produces a 22.5 kDa recombinant protein (Nf-profilin-His). The profilin gene of pathogenic *N. fowleri* exhibited 83% homology with that of *N. gruberi* (non-pathogenic

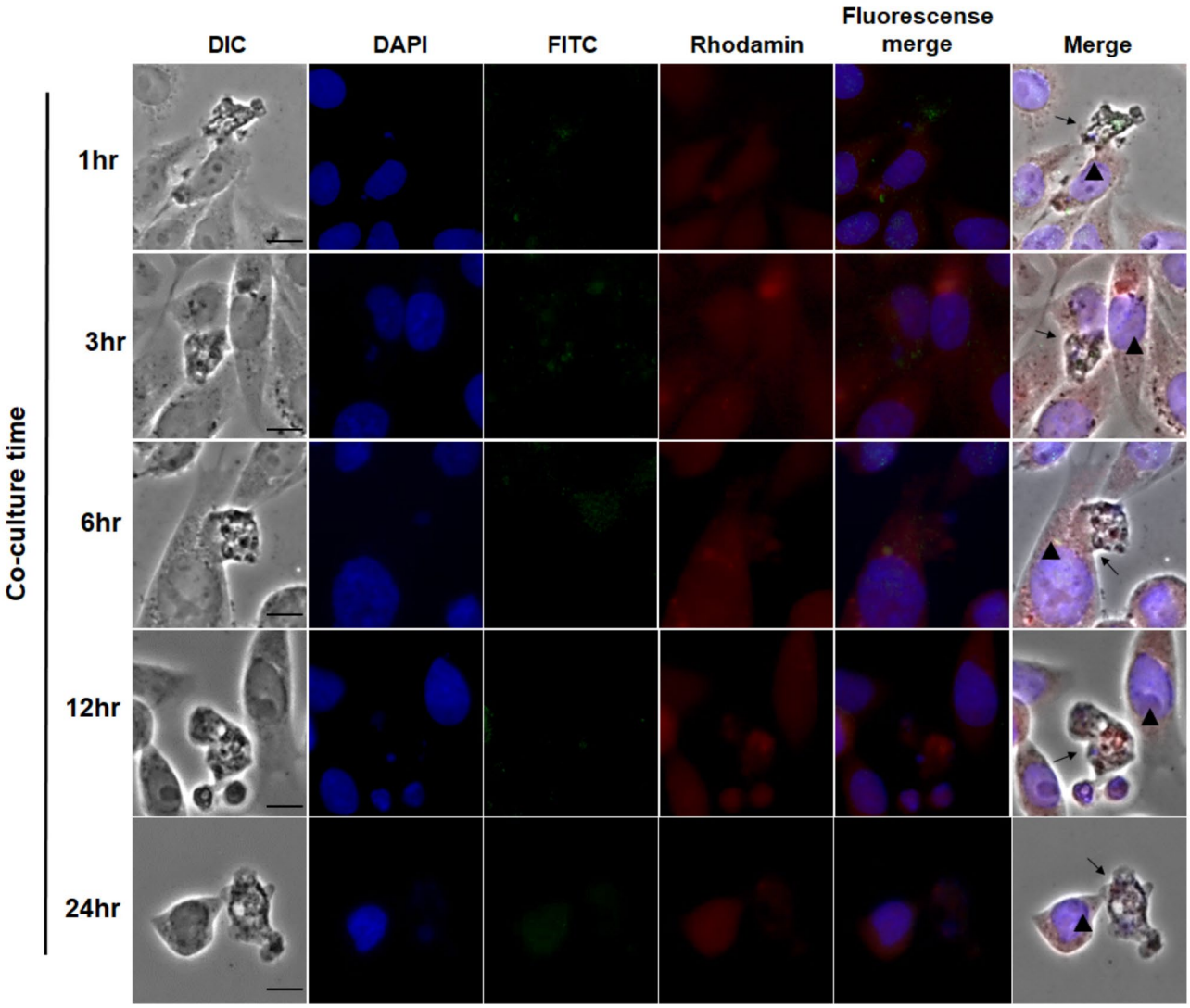

Fig. 11. Localization of Nf-profilin protein in *N. fowleri* trophozoites co-cultured with CHO cells by immunofluorescence assay (× 400). Arrows, *N. fowleri* cysts and trophozoites; Arrow head, CHO cells. Scale bar, 20 μm.

amoebae), 33% homology with its close relative species, *Acanthamoeba castellanii*, and 18% homology with the human profilin gene. RT-PCR results confirmed that *nf-profilin* expression is higher in cysts than in trophozoites, whereas *nf-actin* expression was significantly higher in trophozoites and low in cysts. Consistent with RT-PCR, Western blotting showed low Nf-profilin expression in trophozoites and a distinct 22.5 kDa band in cysts. Immunocytochemistry analysis revealed that Nf-profilin weakly localized to the pseudopodia and cytoplasm in trophozoites, while it was not detected in phagocytic structures such as food-cups or amoebastomes. This suggests Nf-profilin may not directly contribute to phagocytic functions of *N. fowleri*. In cysts, which do not engage in phagocytosis, Nf-profilin was distributed throughout the cytoplasm. These findings indicate that as *N. fowleri* transitions from cyst to trophozoite, Nf-profilin expression decreases.

Time-course observations in *N. fowleri* co-cultured with CHO cells showed morphological changes with increased co-culture duration. After one hour, trophozoites exhibited amoeboid movement, attaching to CHO cells and rapidly performing phagocytosis, resulting in a decrease in CHO cell numbers and increased amoebic proliferation. In cysts, slight floating was observed after one hour, but after three hours, pre-cyst forms developed protruded pseudopodia. After twelve hours, numerous amoebae had transitioned to trophozoites with active pseudopodia and food-cups, resulting in a significant reduction in CHO cell numbers. RT-PCR analysis of *nf-profilin* gene expression in co-cultured cysts and trophozoites demonstrated that *nf-profilin* expression was highest in cysts at one hour, decreasing as the co-culture continued, indicating a transition to the trophozoite form. RT-qPCR quantification showed that at one hour, *nf-profilin* expression was over 2.5 times higher in cysts than in trophozoites. These results indicate that *nf-profilin* is more highly expressed in cysts than in trophozoites. The difference in expression levels of *nf-profilin* and *nf-actin* between trophozoites and cysts may be related to the amoeba's transition from cysts to trophozoites when target cells are present, and the formation of food-cup

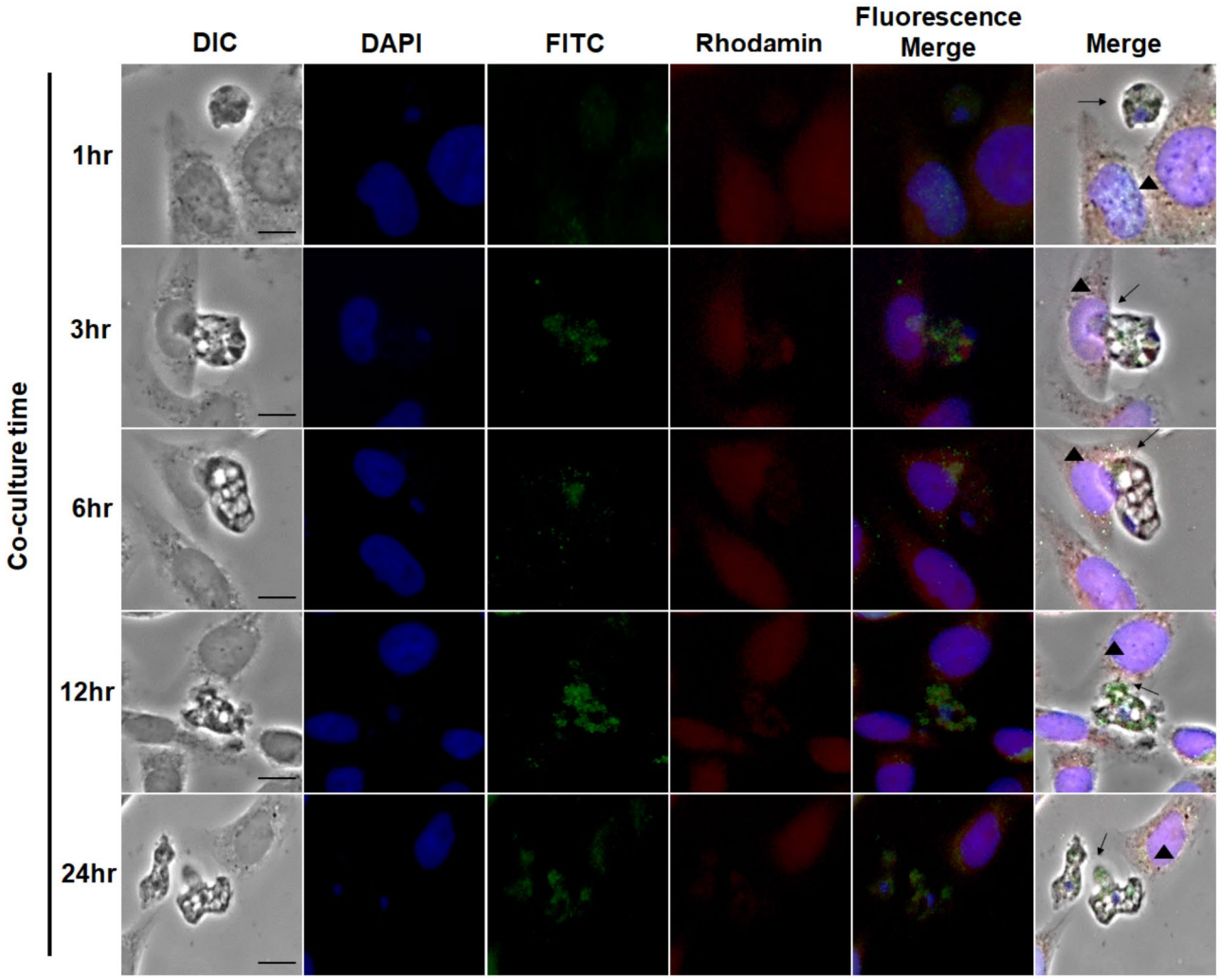

Fig. 12. Localization of Nf-actin protein in *N. fowleri* cysts co-cultured with CHO cells by immunofluorescence assay (× 400). Arrows, *N. fowleri* cysts and trophozoites; Arrow head, CHO cells. Scale bar, 20 μm.

structures (amoebastome) to initiate phagocytosis. Further localization analysis using immunofluorescence found that in cystic amoebae, Nf-profilin initially distributed throughout the cytoplasm, with CHO cells distinguished by SNARF-red staining and Nf-profilin visualized via green fluorescence. After three hours, pseudopodia began forming in cysts, directed toward CHO cells, with Nf-profilin concentrating within the cell. By six hours, in fully developed trophozoites, Nf-profilin was concentrated in specific regions, such as pseudopodia or food-cups, with further decreased expression. In our result, it seems that the mRNA levels of Nf-profilin are higher than the protein levels of Nf-profilin observed in the immunofluorescence assays for trophozoites. Some reasons for the differences between mRNA and protein expression levels are post-transcriptional regulation, protein level regulation, and post-translational modifications. The complex regulatory mechanisms in the process from mRNA to protein lead to differences between mRNA and protein expression levels, allowing cells to respond quickly and precisely to environmental changes.

Actin plays a critical role in protozoan cellular functions, including survival, motility, and environmental interaction[41–44]. Actin filaments polymerize at pseudopodial leading edges, enabling movement and forming phagocytic cups for particle engulfment[45,46]. The *Nf-actin* supports host tissue penetration, immune evasion, and pathogen spread[14,20]. Comparative experiments with Nf-actin showed minimal expression in cysts co-cultured with CHO cells for one hour, but after three hours, Nf-actin expression increased in amoebae transitioning to trophozoites. Over time, Nf-actin expression strengthened in food-cups and amoebastomes adhering to CHO cells. Confocal microscopy confirmed that Nf-profilin was strongly expressed in cysts and weakly expressed near the nucleus and pseudopodia tips after six hours in trophozoites (Fig. S1). In contrast, Nf-actin expression intensified in food-cups or amoebastomes in trophozoites adhering to target cells.

In conclusion, Nf-profilin is highly expressed in cysts, reflecting a dormant state with limited motility and phagocytosis, while expression decreases as the amoeba transitions to trophozoites. Conversely, Nf-actin is scarcely expressed in cysts but increases as amoebae transform into trophozoites and interact with target cells,

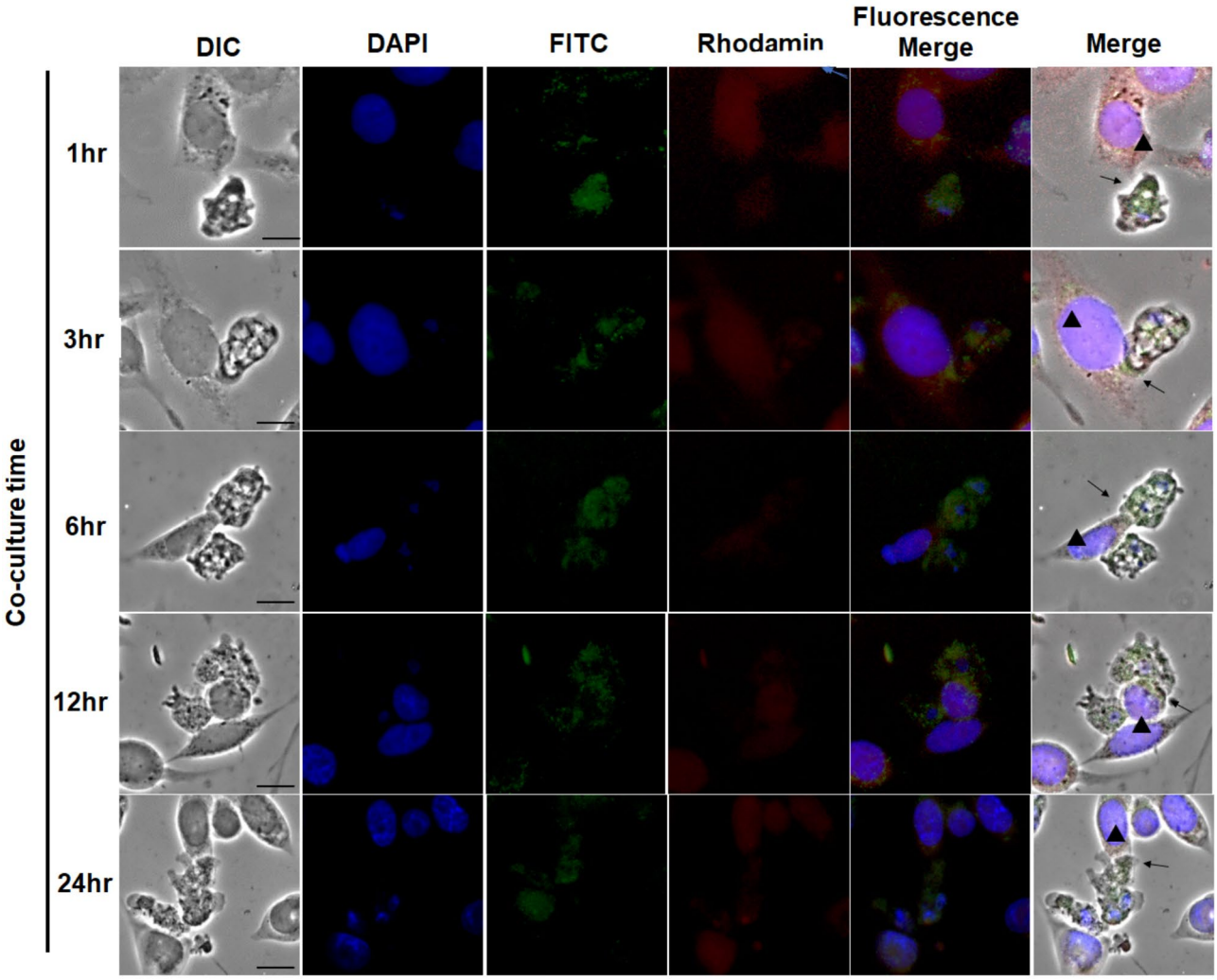

Fig. 13. Localization of Nf-actin protein in *N. fowleri* trophozoites co-cultured with CHO cells by immunofluorescence assay (× 400). Arrows, *N. fowleri* cysts and trophozoites; Arrow head, CHO cells. Scale bar, 20 μm.

with strong expression in pseudopods and food-cup structures. These results suggest Nf-profilin is not directly involved in adhesion and phagocytosis, whereas Nf-actin plays a key role in these processes. Both Nf-actin and Nf-profilin are crucial for the dynamic regulation of actin filaments. Studying Nf-profilin regulation may serve as a foundation for exploring *N. fowleri* pathogenicity and developing treatments.

Methods

Culture and encystation of *N. fowleri*

N. fowleri trophozoites (Carter NF69; ATCC No. 30215) were axenically cultured in Nelson's medium containing 5% fetal bovine serum (FBS) at 37 °C. Cyst formation was induced following previously described methods with modifications. Briefly, *N. fowleri* trophozoites were washed twice with phosphate-buffered saline (PBS), centrifuged at 1500 rpm for 3 min, and then placed into a 6-well plate with incomplete Nelson's medium for 18 h. To induce starvation, the cells were washed twice with PBS and transferred to encystment medium. After a 10 h incubation in the encystment medium, the *N. fowleri* cysts were observed under an inverted microscope and harvested by centrifugation.

Cultivation of target cells

The target cells, Chinese hamster ovary (CHO) cells, were cultured in Dulbecco's Modified Eagle Medium (DMEM) at 37 °C in a 5% CO_2 incubator. CHO cells were grown in 75-cm^2 flasks until a monolayer was formed. The cells were then detached using 5 ml of trypsin-EDTA solution, washed twice with PBS, and seeded in 6-well plates at a density of 5×10^5 cells/ml. Monolayer-cultured CHO cells were used for all experiments.

Gene cloning and sequence analysis
In a previous study, we identified the differentially expressed *nf-profilin* gene in *N. fowleri* cysts and trophozoites using RNA-seq. To amplify the DNA by PCR, primers for the *nf-profilin* gene were designed based on the transcriptome data of *N. fowleri* (nf-profilin F: ATGGTACCAGCTTGCTCCAA, R: GCTCTGCAACATCAC ACAGA). The PCR product was subcloned for sequence analysis and to produce Nf-profilin-(6xHis) fusion protein in a pET30a vector.

Recombinant Nf-profilin expression and purification
An overnight culture of *Escherichia coli* cells containing the pET30a/nf-profilin construct was diluted 1:100 in LB medium supplemented with ampicillin and chloramphenicol and incubated until the optical density at 600 nm (OD600) reached 0.5–0.8. Protein expression was induced using isopropyl β-D-thiogalactopyranoside (IPTG), followed by a 6 h growth period. The cells were harvested, sonicated, treated with RNase and DNase, and centrifuged to remove debris. Recombinant Nf-profilin was purified using Ni-NTA resin, and the eluted proteins were concentrated using Amicon Ultra-15 filters (Millipore, Bedford, MA, USA).

Production of anti-nf-profilin monoclonal antibodies
Monoclonal antibodies were produced using methods described by Sohn et al.[14]. Briefly, 50 μg of Nf-profilin protein was mixed with 100 μg of Freund's complete adjuvant (Sigma Chemical Co., St. Louis, MO, USA) and injected intraperitoneally into 6-week-old female Balb/c mice. Two subsequent boosts with 25 μg of protein mixed with Freund's incomplete adjuvant (Sigma Chemical Co.) were administered. Antibody production was assessed by ELISA using blood samples collected from the caudal vein. A final boost was given 5 days before cell fusion. For hybridoma production, splenocytes from immunized mice were fused with myeloma cells in DMEM containing PEG. Hybridoma cells were cultured in HAT medium, selected, and cloned by limiting dilution. Monoclonal antibody-producing clones were expanded, and ascitic fluid was collected from mice injected with these clones. The antibodies were purified using a Protein A column, concentrated using Amicon Ultra tubes, and stored at -20 °C until use.

Immunofluorescence assay
The localization of Nf-profilin in *N. fowleri* was assessed using an immunofluorescence assay. *N. fowleri* and CHO cells were fixed in 10% formalin in 0.9% saline for 10 min at room temperature. Cells were washed twice with PBS, permeabilized with 1% ammonium hydroxide for 5 min at room temperature, and washed with 0.05% Tween-20 and saline. After blocking with 3% bovine serum albumin (BSA) in PBST, the cells were incubated overnight at 4 °C with either anti-nf-profilin monoclonal antibodies or nf-actin antibodies (diluted 1:100 in 3% BSA). Following several PBS washes, the cells were incubated with fluorescein isothiocyanate (FITC)-conjugated anti-mouse antibodies (Sigma Chemical Co.) diluted 1:100 for 2 h at 4 °C. CHO cells were stained with 10 μM 5-(and 6)-chloromethyl SNARF-1 (Molecular Probes, Eugene, OR, USA) for 30 min at 37 °C in a 5% CO_2 incubator to label live cells. Cell fluorescence was examined using either an Axiovert 200 M microscope or an LSM710 confocal microscope (Carl Zeiss GmbH, Jena, Germany). Images were processed using Adobe Photoshop 7.0 software.

cDNA synthesis and reverse transcription PCR
Total RNA was extracted from *N. fowleri* samples using an RNeasy® Mini kit (Qiagen, Hilden, Germany). For cDNA synthesis, 5 μg of total RNA was reverse-transcribed using oligo(dT) primers. The reaction was incubated at 42 °C for 1 h, followed by a denaturation step at 94 °C for 5 min, and then held at 4 °C. Reverse transcription PCR (RT-PCR) was performed using primers specific for the *nf-profilin* gene. The PCR conditions were: initial denaturation at 95 °C for 5 min, followed by 35 cycles of denaturation at 95 °C for 30 s, annealing at 57 °C for 30 s, extension at 72 °C for 30 s, and a final extension at 72 °C for 10 min. Real-time RT-PCR was used to quantify *nf-profilin* gene expression in *N. fowleri* co-cultured with target cells. qRT-PCR was performed using a QuantStudio 5 Real-Time PCR System (Thermo Fisher Scientific, Waltham, MA, USA) with SYBR Premix Ex Taq (Tli RNaseH Plus; RR420) (Takara Bio Inc., Shiga, Japan). All qRT-PCR reactions were run in duplicate, and individual gene amplification signals were normalized to *N. fowleri* glyceraldehyde-3-phosphate dehydrogenase (NfGAPDH).

Statistical analysis
All experiments were performed in triplicate to ensure reproducibility. Statistical differences between groups or samples were analyzed using the Student's t-test, with significance set at $p < 0.05$.

Data availability
The data generated during the current study are available from the corresponding author upon reasonable request.

Received: 7 November 2024; Accepted: 11 February 2025
Published online: 27 February 2025

References
1. Fowler, M. & Carter, R. F. Acute pyogenic meningitis probably due to *Acanthamoeba* sp.: A preliminary report. *Br. Med. J.* **2**, 740–742. https://doi.org/10.1136/bmj.2.5464.734-a (1965).
2. Martinez, A. J. & Visvesvara, G. S. Free-living, amphizoic and opportunistic amebas. *Brain Pathol.* **7**, 583–598. https://doi.org/10.1111/j.1750-3639.1997.tb01076.x (1997).

3. Tyndall, R. L. et al. Effect of thermal additions on the density and distribution of thermophilic amoebae and pathogenic *Naegleria fowleri* in a newly created cooling lake. *Appl. Environ. Microbiol.* **55**, 722–732. https://doi.org/10.1128/aem.55.3.722-732.1989 (1989).
4. Visvesvara, G. S., Moura, H. & Schuster, F. L. Pathogenic and opportunistic free-living amoebae: *Acanthamoeba* spp., *Balamuthia mandrillaris*, *Naegleria fowleri*, and *Sappinia diploidea*. *FEMS Immunol. Med. Microbiol.* **50**, 1–26. https://doi.org/10.1111/j.1574-695X.2007.00232.x (2007).
5. Moseman, E. A. Battling brain-eating amoeba: enigmas surrounding immunity to *Naegleria fowleri*. *PLoS Pathog.* **16**, e1008406. https://doi.org/10.1371/journal.ppat.1008406 (2020).
6. Sarah, S., Long, C. G. P. & Fischer, M. David Kimberlin. *Principles and Practice of Pediatric Infectious Diseases* (2022).
7. Marciano-Cabral, F. & Cabral, G. A. The immune response to *Naegleria fowleri* amebae and pathogenesis of infection. *FEMS Immunol. Med. Microbiol.* **51**, 243–259. https://doi.org/10.1111/j.1574-695X.2007.00332.x (2007).
8. Jahangeer, M. et al. *Naegleria fowleri*: sources of infection, pathophysiology, diagnosis, and management; a review. *Clin. Exp. Pharmacol. Physiol.* **47**, 199–212. https://doi.org/10.1111/1440-1681.13192 (2020).
9. Schuster, F. L. & Visvesvara, G. S. Free-living amoebae as opportunistic and non-opportunistic pathogens of humans and animals. *Int. J. Parasitol.* **34**, 1001–1027. https://doi.org/10.1016/j.ijpara.2004.06.004 (2004).
10. Martinez, D. Y. et al. Successful treatment of *Balamuthia mandrillaris* amoebic infection with extensive neurological and cutaneous involvement. *Clin. Infect. Dis.* **51**, e7–11. https://doi.org/10.1086/653609 (2010).
11. Stevens, A. R., Shulman, S. T., Lansen, T. A., Cichon, M. J. & Willaert, E. Primary amoebic meningoencephalitis: A report of two cases and antibiotic and immunologic studies. *J. Infect. Dis.* **143**, 193–199. https://doi.org/10.1093/infdis/143.2.193 (1981).
12. Kim, J. H. et al. Effect of therapeutic chemical agents in vitro and on experimental meningoencephalitis due to *Naegleria fowleri*. *Antimicrob. Agents Chemother.* **52**, 4010–4016. https://doi.org/10.1128/AAC.00197-08 (2008).
13. Pugh, J. J. & Levy, R. A. *Naegleria fowleri*: Diagnosis, pathophysiology of brain inflammation, and antimicrobial treatments. *ACS Chem. Neurosci.* **7**, 1178–1179. https://doi.org/10.1021/acschemneuro.6b00232 (2016).
14. Sohn, H. J., Kim, J. H., Shin, M. H., Song, K. J. & Shin, H. J. The Nf-actin gene is an important factor for food-cup formation and cytotoxicity of pathogenic *Naegleria fowleri*. *Parasitol. Res.* **106**, 917–924. https://doi.org/10.1007/s00436-010-1760-y (2010).
15. Chávez-Munguía, B. et al. *Naegleria fowleri*: Contact-dependent secretion of electrondense granules (EDG). *Exp. Parasitol.* **142**, 1–6 (2014).
16. Gutierrez-Sanchez, M., Carrasco-Yepez, M. M., Herrera-Diaz, J. & Rojas-Hernandez, S. Identification of differential protein recognition pattern between *Naegleria fowleri* and *Naegleria lovaniensis*. *Parasite Immunol.* **42**, e12715. https://doi.org/10.1111/pim.12715 (2020).
17. SHIN, H. J. et al. Molecular cloning and characterization of a gene encoding a 13.1 kDa antigenic protein of *Naegleria fowleri*. *J. Eukaryot. Microbiol.* **48**, 713–717 (2001).
18. Song, K. J. et al. Molecular cloning and characterization of a cytosolic heat shock protein 70 from *Naegleria fowleri*. *Parasitol. Res.* **100**, 1083–1089. https://doi.org/10.1007/s00436-006-0404-8 (2007).
19. Shin, H. J. The nfa1 gene contributed on the contact-dependent pathogenic mechanisms of *Naegleria fowleri*. *Hanyang Med. Rev.* **30**, 204–212 (2010).
20. Sohn, H. J. et al. Cellular characterization of actin gene concerned with contact-dependent mechanisms in *Naegleria fowleri*. *Parasite Immunol.* **41**, e12631 (2019).
21. Kim, J. H., Kim, D. & Shin, H. J. Contact-independent cell death of human microglial cells due to pathogenic Naegleria fowleri trophozoites. *Korean J. Parasitol.* **46**, 217–221. https://doi.org/10.3347/kjp.2008.46.4.217 (2008).
22. Kim, J. H. et al. Immunodominant antigens in Naegleria fowleri excretory–secretory proteins were potential pathogenic factors. *Parasitol. Res.* **105**, 1675–1681. https://doi.org/10.1007/s00436-009-1610-y (2009).
23. Sohn, H. J., Kim, J. H., Kim, K., Park, S. & Shin, H. J. De Novo Transcriptome profiling of *Naegleria fowleri* trophozoites and cysts via RNA sequencing. *Pathogens* **12** https://doi.org/10.3390/pathogens12020174 (2023).
24. Carlsson, L., Nyström, L. E., Sundkvist, I., Markey, F. & Lindberg, U. Actin polymerizability is influenced by profilin, a low molecular weight protein in non-muscle cells. *J. Mol. Biol.* **115**, 465–483 (1977).
25. Schutt, C. E., Myslik, J. C., Rozycki, M. D., Goonesekere, N. C. & Lindberg, U. The structure of crystalline profilin-β-actin. *Nature* **365**, 810–816 (1993).
26. Lappalainen, P., Kotila, T., Jegou, A. & Romet-Lemonne, G. Biochemical and mechanical regulation of actin dynamics. *Nat. Rev. Mol. Cell. Biol.* **23**, 836–852. https://doi.org/10.1038/s41580-022-00508-4 (2022).
27. Hartwig, J. H., Chambers, K. A., Hopcia, K. L. & Kwiatkowski, D. J. Association of profilin with filament-free regions of human leukocyte and platelet membranes and reversible membrane binding during platelet activation. *J. Cell. Biol.* **109**, 1571–1579. https://doi.org/10.1083/jcb.109.4.1571 (1989).
28. Buss, F., Temm-Grove, C., Henning, S. & Jockusch, B. M. Distribution of profilin in fibroblasts correlates with the presence of highly dynamic actin filaments. *Cell. Motil. Cytoskeleton.* **22**, 51–61. https://doi.org/10.1002/cm.970220106 (1992).
29. Alvarado, M. et al. Profilin as a severe food allergen in allergic patients overexposed to grass pollen. *Allergy* **69**, 1610–1616 (2014).
30. Gunning, P. W., Ghoshdastider, U., Whitaker, S., Popp, D. & Robinson, R. C. The evolution of compositionally and functionally distinct actin filaments. *J. Cell Sci.* **128**, 2009–2019 (2015).
31. Sohn, H. J. et al. Efficient liquid media for encystation of pathogenic free-living amoebae. *Korean J. Parasitol.* **55**, 233–238. https://doi.org/10.3347/kjp.2017.55.3.233 (2017).
32. Marciano-Cabral, F. Biology of Naegleria spp. *Microbiol. Rev.* **52**, 114–133. https://doi.org/10.1128/mr.52.1.114-133.1988 (1988).
33. Hamaty, E. Jr et al. A fatal case of primary amoebic meningoencephalitis from recreational waters. *Case Rep. Crit. Care* 9235794 (2020).
34. Siddiqui, R., Ali, I. K. M., Cope, J. R. & Khan, N. A. Biology and pathogenesis of *Naegleria fowleri*. *Acta Trop.* **164**, 375–394 (2016).
35. Cho, M. S. et al. Immunological characterizations of a cloned 13.1-kilodalton protein from pathogenic Naegleria fowleri. *Clin. Diagn. Lab. Immunol.* **10**, 954–959. https://doi.org/10.1128/cdli.10.5.954-959.2003 (2003).
36. Song, K. J. et al. Heat shock protein 70 of Naegleria fowleri is important factor for proliferation and in vitro cytotoxicity. *Parasitol. Res.* **103**, 313–317. https://doi.org/10.1007/s00436-008-0972-x (2008).
37. Moon, E. K., Chung, D. I., Hong, Y. C. & Kong, H. H. Autophagy protein 8 mediating autophagosome in encysting Acanthamoeba. *Mol. Biochem. Parasitol.* **168**, 43–48. https://doi.org/10.1016/j.molbiopara.2009.06.005 (2009).
38. Pantaloni, D., Clainche, C. L. & Carlier, M. F. Mechanism of actin-based motility. *Science* **292**, 1502–1506 (2001).
39. Pollard, T. D. & Borisy, G. G. Cellular motility driven by assembly and disassembly of actin filaments. *Cell* **112**, 453–465 (2003).
40. Witke, W. The role of profilin complexes in cell motility and other cellular processes. *Trends Cell Biol.* **14**, 461–469 (2004).
41. Glotzer, M. The molecular requirements for cytokinesis. *Science* **307**, 1735–1739 (2005).
42. Pomorski, P. et al. Actin dynamics in Amoeba proteus motility. *Protoplasma* **231**, 31–41. https://doi.org/10.1007/s00709-007-0243-1 (2007).
43. Hancock, W. O. Bidirectional cargo transport: Moving beyond tug of war. *Nat. Rev. Mol. Cell Biol.* **15**, 615–628 (2014).
44. Schaks, M., Giannone, G. & Rottner, K. Actin dynamics in cell migration. *Essays Biochem.* **63**, 483–495 (2019).
45. Pollard, T. D. & Cooper, J. A. Actin, a central player in cell shape and movement. *Science* **326**, 1208–1212 (2009).
46. Uribe-Querol, E. & Rosales, C. Phagocytosis: Our current understanding of a universal biological process. *Front. Immunol.* **11**, 1066 (2020).

Acknowledgements
This work was supported by the National Research Foundation of Korea (NRF) grant funded by the Korea government (MSIT) (NRF-2021R1C1C2009518).

Author contributions
H-J Sohn conceived and designed the experiments. H-J Sohn, A-J Ham, A-Y Park, and J-H Lee; Investigation, Methodology. H-J Sohn, A-J Ham, and S Park; Software and Validation. H-J Sohn and H-J Shin; Visualization. S Park, H-J Shin, and J-H Kim helped with many discussions. H-J Sohn wrote the original manuscript. J-H Kim supervised and provided critical feedback. All authors commented on the original manuscript.

Declarations

Competing interests
The authors declare no competing interests.

Additional information
Supplementary Information The online version contains supplementary material available at https://doi.org/10.1038/s41598-025-90222-w.

Correspondence and requests for materials should be addressed to J.-H.K.

Reprints and permissions information is available at www.nature.com/reprints.

Publisher's note Springer Nature remains neutral with regard to jurisdictional claims in published maps and institutional affiliations.